

This work was written as part of one of the author's official duties as an Employee of the United States Government and is therefore a work of the United States Government. In accordance with 17 U.S.C. 105, no copyright protection is available for such works under U.S. Law. Access to this work was provided by the University of Maryland, Baltimore County (UMBC) ScholarWorks@UMBC digital repository on the Maryland Shared Open Access (MD-SOAR) platform.

Please provide feedback

Please support the ScholarWorks@UMBC repository by emailing scholarworks-group@umbc.edu and telling us what having access to this work means to you and why it's important to you. Thank you.

Impact of Nonlinearity on RF-Modulated Frequency Combs with Different Modulation Depths in an MUTC Photodetector

Seyed Ehsan Jamali Mahabadi, Thomas F. Carruthers,
and Curtis R. Menyuk

Computer Science and Electrical Engineering Department,
University of Maryland, Baltimore County
Baltimore, MD 21250 USA
sjamali1@umbc.edu

Meredith N. Hutchinson, Jason D. McKinney,
and Keith J. Williams

U.S. Naval Research Laboratory
Washington, DC 20375 USA

Abstract—We calculate the impact of nonlinearity in a modified uni-traveling carrier (MUTC) photodetector on an RF-modulated frequency comb that is generated using short optical pulses. We take into account bleaching (nonlinear saturation), which plays an important role due to the large peak-to-average power ratio. Nonlinear impairment of an RF-modulated continuous wave is characterized by the second- and third-order intermodulation distortion (IMD2 and IMD3). By contrast, an RF-modulated frequency comb is characterized by a distinct IMD2_n and IMD3_n for each comb line n . We study the effect of modulation depth on nonlinearity in frequency combs, comparing modulation depths of 4% and 8%. When we include bleaching, we find that the OIP3_n , third-order intercept point for the n -th comb line, increases when the modulation depth increases for comb lines at frequencies above 2 GHz ($n \geq 40$), so that distortion decreases. We show that this effect occurs because bleaching attenuates lower frequencies more than higher frequencies and this preferential attenuation increases as the modulation depth increases.

Index Terms—nonlinearity, MUTC, frequency comb, IMD2, IMD3, bleaching

I. INTRODUCTION

Optical links are an appealing choice in a variety of applications [1]. Applications include antenna remoting [2], radio-over fiber [3], beamforming in phased-array radars [4], and optical signal processing of microwave signals [5]. These applications push link lengths towards 100 km or more. For link lengths in this range, stimulated Brillouin scattering [6] (SBS) severely limits the optical launch power, which necessitates inclusion of either midspan or post-link optical amplification [7]. In many cases (e.g., antenna remoting), midspan amplification is not an option; the use of an amplifier prior to the photodetector drives the link noise figure substantially above the shot-noise limit [7]. Optical links also have some limitations such as lower efficiency, higher noise figure, lower spur-free dynamic range (SFDR), and lower output RF power in comparison to purely electronic systems [8]. While any single CW optical signal is limited to powers below the

threshold power for SBS, additional signals outside the SBS gain bandwidth may be launched into the fiber without penalty. Hence, broadband digital signals are less susceptible to the effects of SBS than are narrowband signals. McKinney *et al.* [7] utilized a broadband optical comb as the optical carrier in a long-haul link architecture. As each comb line experiences the same RF modulation, the optical comb effectively behaves as an N -element array in the absence of chromatic dispersion. The RF signals that are recovered from the heterodyne beat of each comb line with its sidebands are coherently summed by the photodetector. Therefore, the comb-based link has the same RF performance as a conventional analog link operating at the same average photocurrent (optical power) level. However, the power in each comb line is now limited by the SBS threshold power. Hence, an optical comb with N comb lines can transfer N -times more average power through the link than is possible in a CW laser-based analog link. This approach reduces the dependence on amplification prior to the photodetector in single-span links and may eventually obviate the need for them [7]. Examples include systems that use frequency combs to generate low-noise microwave signals [9] and systems that use frequency combs to disambiguate radar signals [10]. Frequency combs are generated in the optical domain by creating a stream of short pulses, using for example a short pulse laser [11] or a continuous wave laser followed by an electro-optic modulator [1]. The pulses in a typical optical pulse train have durations less than 500 fs, and are separated by 10–50 ns, corresponding to a repetition rate of 20 MHz to 100 MHz.

In work submitted elsewhere [12], we considered the effect of bleaching (nonlinear saturation) on RF-modulated frequency combs. Here, we consider the impact of nonlinearity on RF-modulated frequency combs with different modulation depths. We calculate the device nonlinearity for the MUTC photodetector with a pulsed optical input. The optical input is a train of short optical pulses with a duration of 100 fs and a repetition frequency of 50 MHz that is modulated at microwave frequencies. In our calculations, the input

Naval Research Laboratory grant number N00173-15-1-G905

p-region	InGaAs, p ⁺ , Zn, 2.0×10^{19} , 50 nm	50 nm
	InP, p ⁺ , Zn, 1.5×10^{18} , 100 nm	150 nm
	InGaAsP, Q1.1, Zn, 2.0×10^{18} , 15 nm	165 nm
	InGaAsP, Q1.4, Zn, 2.0×10^{18} , 15 nm	180 nm
	InGaAs, p, Zn, 2.0×10^{18} , 100 nm	280 nm
	InGaAs, p, Zn, 1.2×10^{18} , 150 nm	430 nm
	InGaAs, p, Zn, 8.0×10^{17} , 200 nm	630 nm
	InGaAs, p, Zn, 5.0×10^{17} , 250 nm	880 nm
i-region	InGaAs, Si, 1.0×10^{16} , 150 nm	1030 nm
	InGaAsP, Q1.4, Si, 1.0×10^{16} , 15 nm	1045 nm
	InGaAsP, Q1.1, Si, 1.0×10^{16} , 15 nm	1060 nm
	InP, Si, 1.4×10^{17} , 50 nm	1110 nm
n-region	InP, Si, 1.0×10^{16} , 900 nm	2010 nm
	InP, n ⁺ , Si, 1.0×10^{18} , 100 nm	2110 nm
	InP, n ⁺ , Si, 1.0×10^{19} , 900 nm	3010 nm
	InGaAs, n ⁺ , Si, 1.0×10^{19} , 20 nm	3030 nm
	InP, n ⁺ , Si, 1.0×10^{19} , 200 nm	3230 nm
InP, semi-insulating substrate Double side polished		

Fig. 1. MUTC photodetector structure.

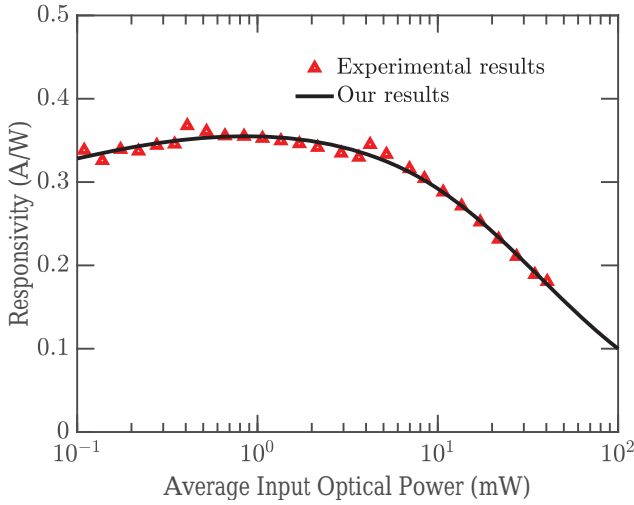


Fig. 2. Responsivity as a function of average input optical power for the MUTC photodetector.

modulation frequencies are $F_1 = 10.0$ MHz, $F_2 = 10.5$ MHz, and $F_3 = 9.0$ MHz. We find that when we include bleaching, the OIP3_n increases when the modulation depth increases at frequencies above 2 GHz ($n \geq 40$). Hence, the distortion decreases with an increase in modulation depth. Bleaching decreases the responsivity, which affects lower frequencies more than higher frequencies and leads to this effect.

Bleaching in a photodetector can occur when optical pulses are detected due to the high peak power of the pulses (10^4 – 10^5 times larger than the average power), and it leads to a reduction in the photodetector's responsivity. This reduction in responsivity can lead to nonlinear distortion of an incoming

RF-photonic signal. Juodawlkis *et al.* [13] have reported that this effect can limit the performance of photonic analog-to-digital converters (PADCs).

We developed an empirical model of the bleaching and incorporated this model into a one-dimensional (1-D) drift-diffusion model that Hu *et al.* [14] previously developed. The bleaching model was based on experimental data that was collected at the Naval Research Laboratory. We then used this model to calculate the nonlinear photodetector responsivity in a modified uni-traveling carrier (MUTC) photodetector. Figure 1 shows the MUTC photodetector structure [15] that we used in our model. With a modulated continuous wave (CW), the device nonlinearity can be characterized using the second- and third-order intermodulation distortions (IMD2 and IMD3) and by the second- and third-order output intercept points (OIP2 and OIP3). This simple characterization is no longer possible when working with frequency combs, since every electrical comb line is impacted by the nonlinearity in a different way. It is necessary to define IMD2_n , IMD3_n , OIP2_n , and OIP3_n for *each* comb line n . We used the three-tone modulation technique [16] to calculate the IMD2_n and IMD3_n in the pulsed mode for modulation depths of 4% and 8% for each comb line n .

The responsivity \mathfrak{R} is the ratio of the output current I_{out} to the input optical power P_{opt} , $\mathfrak{R} = I_{\text{out}}/P_{\text{opt}}$ [17]. The optical generation rate in the drift-diffusion equations is given by

$$G_{\text{opt}} = A G_c \exp[-\alpha(L - x)], \quad (1)$$

where A is the bleaching coefficient as a function of average input optical power that we calculated, G_{opt} is the optical generation rate, G_c is the generation rate coefficient when bleaching is absent, α is the absorption coefficient, x is distance across the device, and L is the device length.

Figure 2 shows experimental results of the responsivity of the MUTC photodetector as a function of the average input optical power with a pulsed input in which pulses have a FWHM duration of 100 fs and a repetition frequency of 50 MHz. In the experiments, a Calmar Mendecino passively-modelocked erbium doped fiber laser was used. The output of the modelocked laser was a train of pulses with a 100-fs FWHM pulse duration and a 50-MHz repetition rate. The output was passed through a variable attenuator and calibrated optical tap with a 90/10 split. The 10% tap was used as a power monitor and the 90% tap illuminated the MUTC photodetector. The average optical power and average photocurrent were measured as the optical attenuator was adjusted. Knowing the repetition rate, the optical power was then converted to a pulse energy to calculate the responsivity. We also show our empirical fit to this data for the MUTC photodetector in pulsed mode.

When considering nonlinearity in photodetectors, IMD3 is particularly significant, since the frequencies that it generates can be close to the fundamental modulation frequencies [18].

Figures 3 and 4 show the fundamental RF output power, the IMD2 power at $F_1 + F_2$, and the IMD3 power at $F_1 + F_2 - F_3$ as functions of the average input optical power. Figure 3 shows

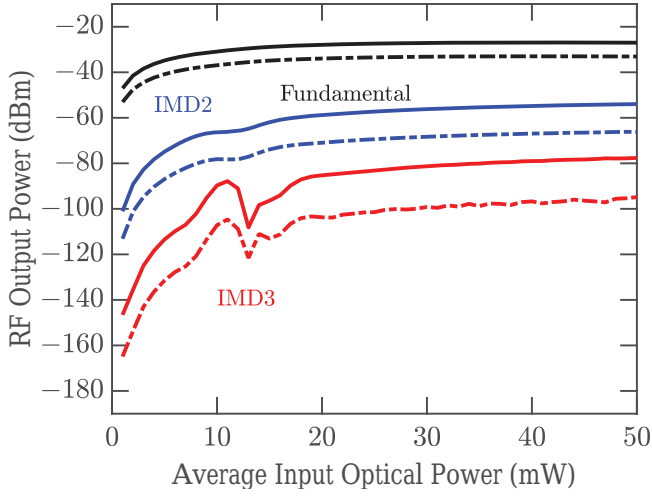


Fig. 3. Power at the fundamental frequency, the IMD2 power, and the IMD3 power for $n = 20$ (1 GHz). The dot-dashed curves show the harmonic powers when the modulation depth is 4%, and the solid curves show the harmonic powers when the modulation depth is 8%.

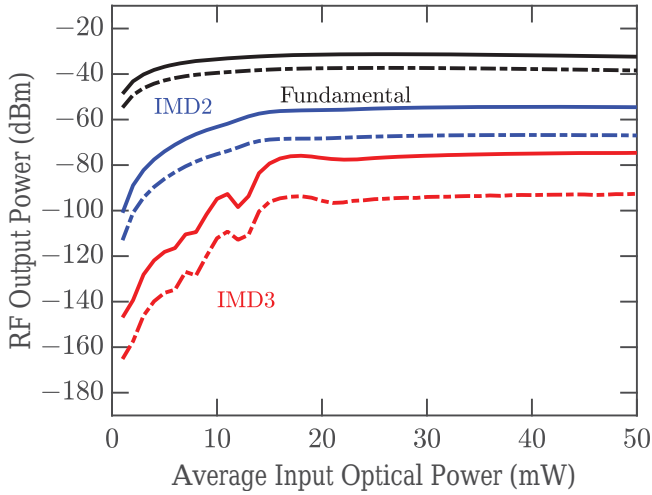


Fig. 4. Power at the fundamental frequency, the IMD2 power, and the IMD3 power for $n = 200$ (10 GHz). The dot-dashed curves show the harmonic powers when the modulation depth is 4%, and the solid curves show the harmonic powers when the modulation depth is 8%.

the $n = 20$ comb line at 1 GHz, and Fig. 4 shows the $n = 200$ comb line at 10 GHz. In Figs. 3 and 4, the dot-dashed curves show the harmonic powers when the modulation depth is 4%, and the solid curves show the harmonic powers when the modulation depth is 8%. As shown in Figs. 3 and 4, the harmonic power values are higher with a modulation depth of 8%. We reported earlier that bleaching reduces the fundamental RF output power [12]. For lower comb line numbers ($n \lesssim 50$) IMD2_n and IMD3_n are larger when bleaching is included, but for higher comb line numbers IMD2_n and IMD3_n are larger when bleaching is not included. Figures 5 and 6 show

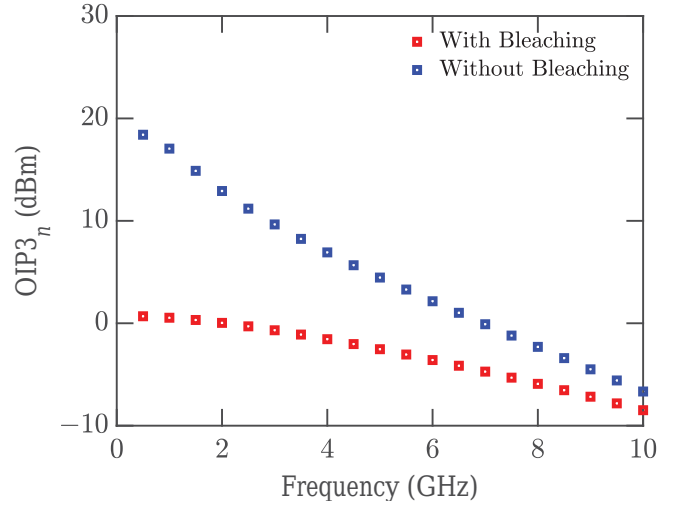


Fig. 5. OIP3_n as a function of frequency for the MUTC photodetector at 25 mW average input optical power for a modulation depth of 4%.

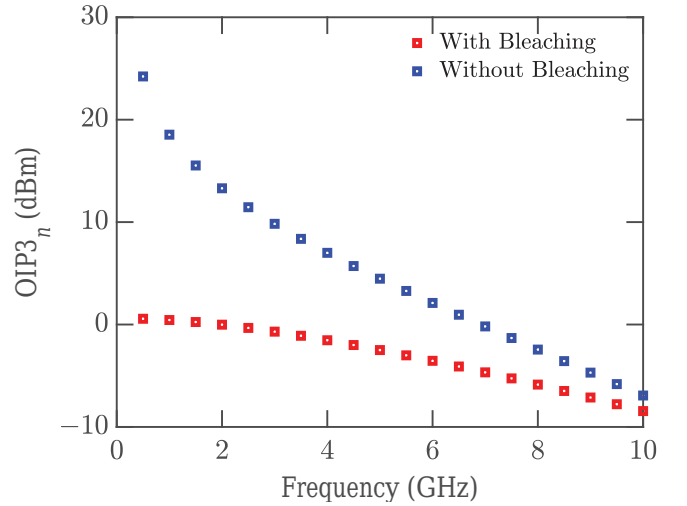


Fig. 6. OIP3_n as a function of frequency for the MUTC photodetector at 25 mW average input optical power for a modulation depth of 8%.

the OIP3_n as a function of frequency at 25 mW average input optical power with and without bleaching for modulation depths of 4% and 8%, respectively. We find that OIP3_n decreases both with and without bleaching, but the decrease is less dramatic when bleaching is taken into account because lower frequency comb lines are impacted more strongly. At frequencies below 2 GHz ($n \lesssim 40$), we find that OIP3_n decreases when the modulation depth increases from 4% to 8%. At frequencies above 2 GHz ($n \gtrsim 40$), the opposite is true. OIP3_n increases when the modulation depth increases. While bleaching lowers the output power at all frequencies, it impacts lower frequencies more than higher frequencies, so that distortion decreases with increased modulation depth at higher frequencies.

In conclusion, we calculate impact of device nonlinearity in an MUTC photodetector on RF-modulated frequency combs as the modulation depth varies. When working with frequency combs, every electrical comb line is impacted by the nonlinearity in a different way, and it is necessary to define $IMD2_n$, $IMD3_n$, $OIP2_n$, and $OIP3_n$ for *each* comb line n . We use the three-tone modulation technique to calculate the $IMD3_n$ for modulation depths of 4% and 8%. We calculate the $OIP3_n$ to characterize the $IMD3_n$. We determine the behavior of $IMD3_n$ and $OIP3_n$ as a function of frequency for different comb lines. $OIP3_n$ decreases both with and without bleaching, but the decrease is less dramatic when bleaching is taken into account because lower frequency comb lines are impacted more strongly. We show that when we include bleaching, the $OIP3_n$ increases when the modulation depth increases at frequencies above 2 GHz ($n \geq 40$). Since the reduced distortion occurs due to a decrease in the responsivity, there will be a negative impact on the signal-to-noise ratio. This issue should be considered in future work.

REFERENCES

- [1] J. D. McKinney and K. J. Williams, "Sampled analog optical links," *IEEE Trans. Microw. Theory Techn.*, vol. 57, pp. 2093–2099, 2009.
- [2] A. J. Seeds and K. J. Williams, "Microwave photonics," *J. Lightw. Technol.* vol. 24, pp. 4628–487, 2002.
- [3] H. Pfrommer, M. A. Piqueras, J. Herrera, V. Polo, A. Martinez, S. Karlsson, O. Kjebon, R. Schatz, Y. Yu, T. Tsegaye, C. P. Liu, C. H. Chuang, A. Enard, F. V. Dijk, A. J. Seeds, and J. Marti, "Full-duplex docsis/wireless docsis fiber-radio network employing packaged afpm-based base-stations," *IEEE Photon. Technol. Lett.* vol. 18, pp. 406–408, 2006.
- [4] D. Dolfi, D. Mongardien, S. Tonda, M. Schaller, and J. Chazelas, "Photonics for airborne phased array radars," in *IEEE Int. Phased Array Syst. Technol. Conf.* pp. 379–382, 2000.
- [5] R. A. Minasian, "Photonic signal processing of microwave signals," *IEEE Trans. Microw. Theory Tech.* vol. 18, pp. 832–846, 2006.
- [6] G. P. Agrawal, *Nonlinear Fiber Optics*. San Diego: Academic Press, 1995.
- [7] J. D. McKinney and V. J. Urick, "Optical comb sources for high dynamic-range single-span long-haul analog optical links," *IEEE Trans. Microw. Theory Techn.* vol. 59, pp. 3249–3257, 2011.
- [8] C. Cox, E. Ackerman, G. Betts, and J. Prince, "Limits on the performance of RF-over-fiber links and their impact on device design," *IEEE Trans. Microw. Theory Techn.* vol. 54, pp. 906–920, 2006.
- [9] J. Millo, R. Boudot, M. Lours, P. Y. Bourgeois, A. N. Luiten, Y. Le Coq, Y. Kersalé, and G. Santarelli, "Ultra-low-noise microwave extraction from fiber-based optical frequency comb," *Opt. Lett.* vol. 34, pp. 3707–3709, 2009.
- [10] S. R. Harmon and J. D. McKinney, "Broadband RF disambiguation in subsampled analog optical links via intentionally-introduced sampling jitter," *Opt. Express* vol. 22, pp. 23928–23937, 2014.
- [11] S. A. Diddams, "The evolving optical frequency comb," *J. Opt. Soc. Am. B* vol. 27, pp. B51–B62, 2010.
- [12] S. E. Jamali Mahabadi, T. F. Carruthers, C. R. Menyuk, M. N. Hutchinson, J. D. McKinney, and K. J. Williams, "Impact of nonlinearity in an MUTC photodetector on an RF-modulated frequency comb," submitted to the 2019 IEEE Photonics Conference.
- [13] P.W. Juodawlkis, F. J. O'Donnell, J. J. Hargreaves, D. C. Oakley, A. Napoleone, S. H. Groves, L. J., Molvar, K. M. Mahoney, L. J. Missaggia, J. P. Donnelly, R.C. Williamson, and J.C. Twichell, "Absorption saturation nonlinearity in InGaAs/InP p-i-n photodiodes," in *15th Annual Meeting of the IEEE Lasers and Electro Optics Society (LEOS)*, vol. 2, pp. 426–427, 2002.
- [14] Y. Hu, C. R. Menyuk, X. Xie, M. N. Hutchinson, V. J. Urick, J. C. Campbell, and K. J. Williams, "Computational study of amplitude-to-phase conversion in a modified untraveling carrier photodetector," *IEEE Photon. J.* vol. 9, 5501111, 2017.
- [15] Z. Li, H. Pan, H. Chen, A. Beling, and J. C. Campbell, "High-saturation-current modified uni-traveling-carrier photodiode with cliff layer," *IEEE J. Quantum Electron.* vol. 46, pp. 626–632, 2010.
- [16] M. N. Draa, A. S. Hastings, and K. J. Williams, "Comparison of photodiode nonlinearity measurement systems," *Opt. Express* vol. 19, pp. 12635–12645, 2011.
- [17] Bahaa E. A. Saleh and Malvin Carl Teich, *Fundamentals of Photonics*. New York: Wiley, 1991.
- [18] H. Pan, Z. Li, A. Beling, and J. C. Campbell, "Measurement and modeling of high-linearity modified uni-traveling carrier photodiode with highly-doped absorber," *Opt. Express*, vol. 17, pp. 20221–20226, 2009.